IOP Conf. Series: Materials Science and Engineering **266** (2017) 012003 doi:10.1088/1757-899X/266/1/012003

Analysis of properties laser welded RAK 40/70 steel sheets

E Evin[1], **M Tomáš**[1] **and M Fujda**[2]

[1] TU Košice, Faculty of Mechanical Engineering, Mäsiarska 74, Košice, Slovakia
[2] TU Košice, Faculty of Materials, Metallurgy and Recycling, Letná 9, Košice, Slovakia

emil.evin@tuke.sk

Abstract. Both, the ecological production and operation of vehicles demand using such materials for deformation zones' structural parts, which show some specific properties and use innovative technologies to process them. Specific requirements for functionality (strength, stiffness, deformation work, fatigue properties) are closely linked to processability (formability). In the paper are presented results for multiphase TRIP steel RAK40/70 when welded by pulse solid-state fiber laser YLS-5000. Based on microstructure analysis in the fusion zone and heat affected zone the welding parameters were optimised. The influence of laser welding on the strength and deformation properties was verified by characteristics of strength, stiffness and deformation work, as they were calculated from mechanical properties measured by tensile test and three-point bending test. The knowledge gathered in the field of laser welding influence on the strength and deformation properties of multiphase TRIP steel RAK40/70 should help designers when design the lightweight structural parts of the car body.

1. Introduction

The automotive industry appears to be a specific branch driven by social pressure to produce more and more safe, economical and environmentally friendly vehicles. From the view of costs, the most effective way to meet the requirements of EU limits for CO_2 95 g to100 km until 2021 is to reduce the car weight [1].

The largest share of the total car weight is the car body - approx. 25% of the vehicle weight. The car body is also the basic part of a car that guarantees passenger safety. One way to reduce the car body weight is modifying the car body structure and replacement the parts made of standard steel by parts made of advanced high strength steels or aluminium alloys, magnesium alloys (even their combination), composites [1]. The steel remains a dominant material for mid-size and compact class cars (B and C segment cars in EU) in the future – Figure 1. For large-size class (D, E and F segment in EU) the aluminium alloy lightweight body concept or a combination of steel and aluminium is applied. For sport cars (S segment in EU) composites are used. The car body weight reduction also offers a promising way to improve car fuel consumption. Furthermore, when the car weight is reduced about 100 kg both, the fuel consumption reduces about 0.3 l/100 km and CO_2 emission reduces about 3.6 g for mid-size cars and 0.4 l/100 km or 4.8 g CO_2 for light trucks. It should be noted, the reduction of both, fuel and energy consumption may not solve the problems of environmental and economic production, operation and disposal of cars throughout their lifecycle. Disposal of steel parts is not

Content from this work may be used under the terms of the Creative Commons Attribution 3.0 licence. Any further distribution of this work must maintain attribution to the author(s) and the title of the work, journal citation and DOI.
Published under licence by IOP Publishing Ltd

problematic. However, the disposal of composite materials and plastics is problematic from an environmental point of view [2].

Today, the car market is influenced by the car silhouette, the lines of edges, the elegance, the dynamic appearance of the body, because there are small differences in the technical equipment of the cars. In addition to design appeal, the car body role is to bear longitudinal, transverse, asymmetrical, bending and torsional loads, without visible signs, and in the event of crash, to mitigate extreme crew overloads to the lowest values and to prevent unwanted parts from entering the crew compartment [3,4]. The results of the SuperLIGHT-CAR project suggest that the application of special structural and safety elements from different types of high-strength steels (DP - Dual Phase, TRIP - Transformation Induced Plasticity, TWIP - Twinning Induced Plasticity, MART - martensitic, F-B Feritic-Bainitic, CP - Complex Phase steels, hot formed bored steels, post forming heat treated steels etc.) can improve the car body safety characteristics and reduce weight by 27% to 38% [5-10].

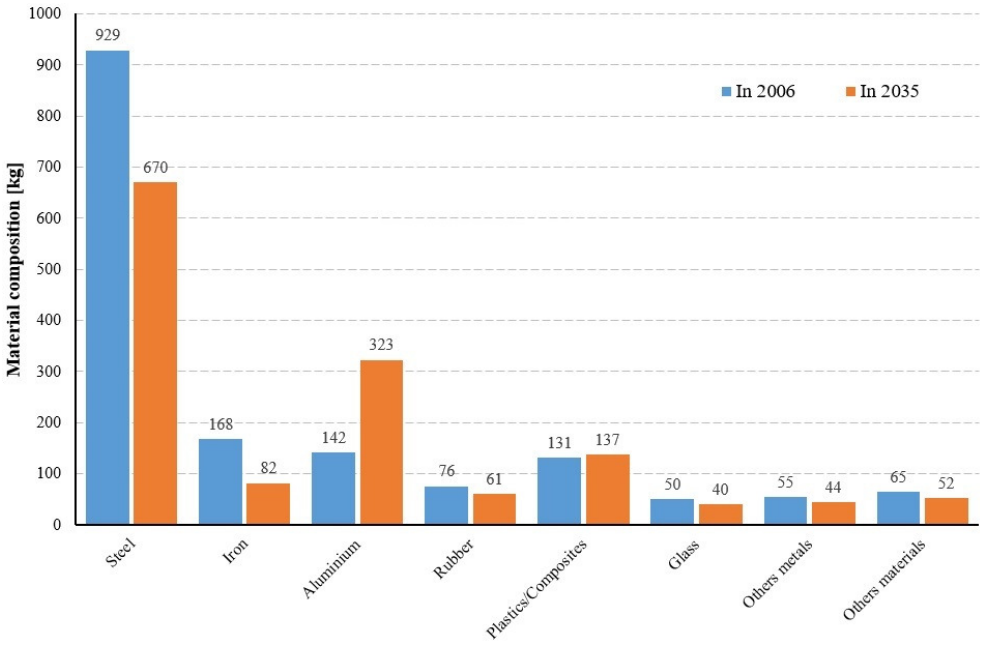


Figure 1. Materials used in automotive production and tendencies to future.

Thanks to their high energy absorption and fatigue strength, TRIP steels are widely applied in the car body deformation zones (transverse and longitudinal body beams, B-pillar reinforcements, or door sills, etc.) [11,12]. TRIP steels are multi-phase steels with transformation-induced plasticity and their microstructure consists of residual austenite islands (5-15%), bainite (25-40%) and martensite possibly scattered in the ferrite matrix (50-60%). When plastically deformed, residual austenite is transformed into martensite (TRIP effect). In order to apply the TRIP effect, a minimum residual austenitic fraction of 5-10% is required. This is ensured by increased carbon and silicon content. In recent years, increased attention has been paid to CMnAl TRIP steels, due to the increased Al content, which causes an increase in C in residual austenite. The same way as Si, Al is also insoluble in cementite, slowing its formation, and at the same time increasing the rate of bainitic transformation. The disadvantage is, Al reduces the effect of hardening of the solid solution against Si and increases the temperature of the M_S. The current development of TRIP steel production is only to partially replace with a limited amount of Al and use 0.05 - 0.10 wt% P. The amount of P used is linked to the Al content because P also suppresses cementite formation and is a very effective element in hardening of the solid solution. Higher levels of silicon and aluminum promote ferrite and bainite formation. These elements are therefore helpful in trying to maintain the required amount of carbon in residual austenite. It is important to suppress the precipitation of carbides during bainitic transformation. For this purpose, silicon and aluminum are used [13].

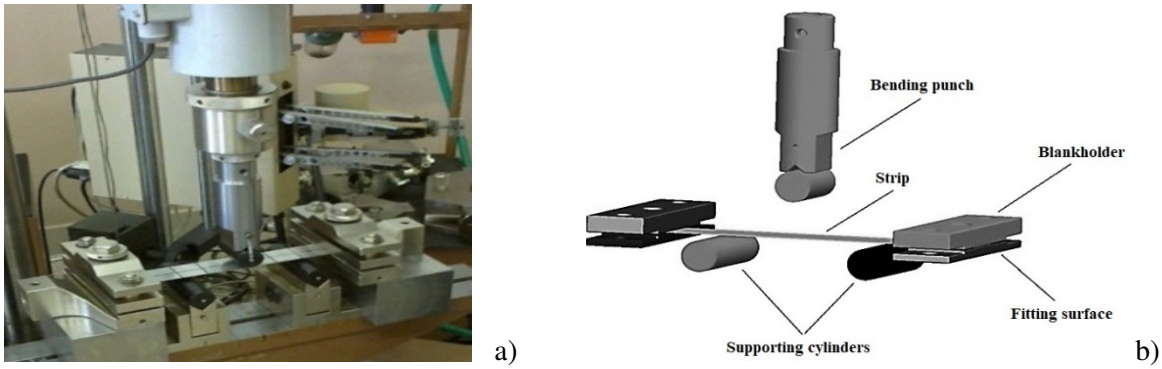
2. Materials and methods used

The experiments were done on multi-phase TRIP steel RAK 40/70 (Residual Austenite, K- Cold rolled, Re/Rm = 400/700). The strength, stiffness, energy absorption ability, formability and weldability have been analyzed from values of mechanical properties measured according to STN EN ISO 6892-1:2010-01; normal anisotropy ratio r measured according to STN EN 10113 and strainhardening exponent n measured according to STN EN 10275. These are shown in the Table 1.

Table 1. Mechanical properties of TRIP steel RAK 40/70 [15,16].

	Dir.	ReH [MPa]	Rm [MPa]	Ag [%]	A [%]	K [MPa]	n [-]	r [-]
BM	0	440	764	25.3	30.3	1497	0.295	0.66
	45	462	761	22.8	26.6	1452	0.275	0.69
	90	457	766	24.3	29.4	1474	0.281	0.62
	Average	453	764	24.1	28.8	1474	0.284	0.66
	Stdev	5	3	0.8	1.5	13	0.004	0.03
LW	0	466	657	20	21	1459	0.249	0.66
	45	483	659	19	20.1	1436	0.235	0.63
	90	474	662	20.3	22.3	1458	0.244	0.60
	Average	474	659	19.8	21.1	1451	0.243	0.63
	Stdev	9	2	1	1	13	0.007	0.03

BM – base material, LW – laser welded



a) b)

Figure 2. The three point bending test: a) fixture, b) scheme.

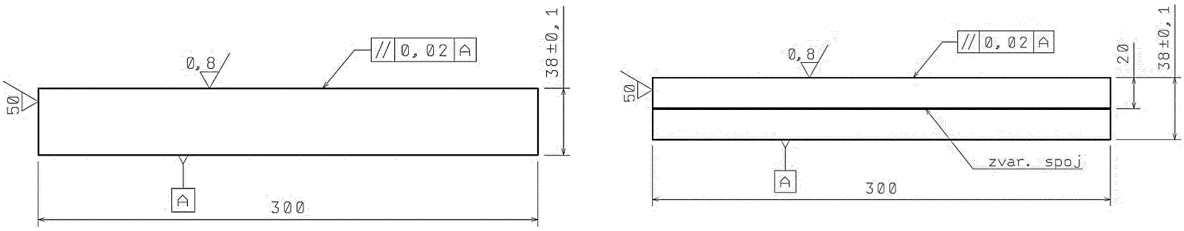


Figure 3. Samples for three point bending test – base material (left), laser welded (right).

The three-point bending test (Figure 2) was used to identify the energy absorption ability and stiffness constant c. Test were performed on samples (Figure 3) from base material (BM) and laser welded one (LW) by pulse solid-state fiber laser YLS-5000 in continuous welding regime. Parameters of laser welding are shown in Table 2 and these were optimized by metallography analysis of microstructure the weld joint (porosity, weld root quality) in the area of fusion zone and heat affected zone. The weldability of base material was evaluated by carbon equivalent calculated from equation (1). The chemical composition of TRIP steel RAK 40/70 measured by atomic emission spectrometry according to ASTM E 415-14 is shown in Table 3 [14].

Table 2. Parameters of laser welding [15,16].

Sheet thickness [mm]	Power [W]	Focal point [mm]	Welding speed [mm.s^{-1}]	Width of FZ [mm]	Width of HAZ [mm]	Note
0.7	2000	10	50	1.05	0.40	Optimal
	2700	10	70	1.17	0.48	

$$C_{ekv} = C + \frac{Mn}{6} + \frac{Cr}{5} + \frac{Ni}{15} + \frac{Mo}{4} + \frac{Cu}{13} + \frac{P}{2} + 0.0024a_0 \quad [wt\ \%] \tag{1}$$

$$C_{ekv} = 0.197 + \frac{1.576}{6} + \frac{0.0445}{5} + \frac{0.016}{15} + \frac{0.022}{4} + \frac{0.022}{13} + \frac{0.015}{2} + 0.0024x0.7 = 0.48 \quad [wt\%]$$

Table 3. Chemical composition of TRIP steel RAK 40/70 [wt%].

C	Si	Mn	P	S	Cu	Al	Cr	Mo	Ni	V	Nb	C_{ekv}
0.197	0.165	1.576	0.015	0.002	0.022	1.352	0.0455	<0.022	0.016	0.0002	0.002	0.48

3. Reached results and discussion

The weld metal microstructure consists predominantly of martensite with a morphology indicating its formation in austenite grains which are elongated in the direction of heat transfer from the center of the weld metal to the base material (Figure 4). The martensite laths in the welded metal are relatively fine and have a random orientation (Figure 4b). The fineness of the martensitic latices increases as the distance from the center line of the weld increases towards the heat-affected zone. Microhardness in the weld metal reached 470 HV0.5. A mixed martensitic-ferritic structure is present in the heat-affected zone of the welding joint (Figure 4c). Microhardness in the heat affected zone reached 450 HV0.5. The proportion of ferrite grains in this mixed microstructure increases as the distance to the base material increases. Close to the base material ferrite prevail in the microstructure of the heat-affected zone in the form of polyhedral grains and martensite in the form of fine shapes of different formation as a minor phase. The microstructure in the base material (Figure 4a) is fine grained, homogeneous with the indications of the layout of the structural components in rows. It consists predominantly of fine grains of ferrite and minority of very fine residual austenite and martensite. Structure also includes granular bainite. Microhardness in the base material reached 222 HV0.5. [15,16]

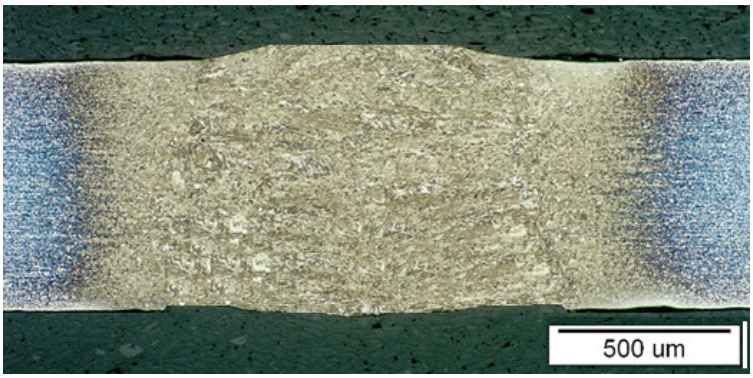


Figure 4. The microstructure of laser weld joint of steel TRIP RAK 40/70.

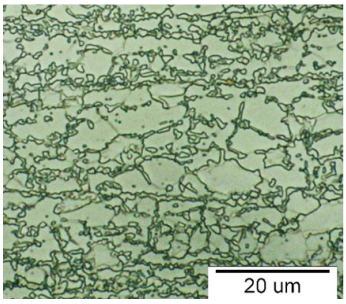


Figure 4a. Detail of the base material.

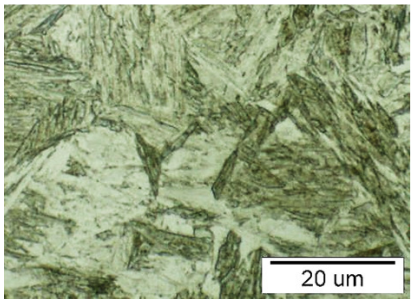


Figure 4b. Detail of the fusion zone.

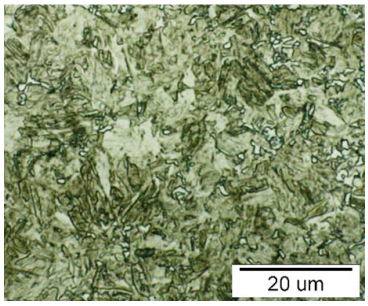
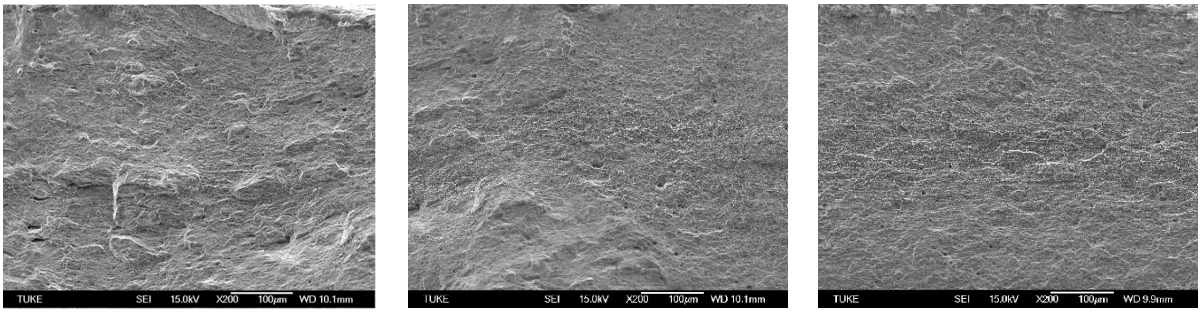


Figure 4c. Detail of the heat affected zone.

The nature of the fracture area of samples broken at the tensile test and the three-point bend was similar. The edges of the fracture surfaces in the weld metal region were poorly deformed in both cases (Figure 5). On their surfaces there are dimples of transcrystalline ductile fracture and relatively smooth areas. In the heat-affected zone of both samples, the fracture surface was less rugged than in the weld metal. They formed predominantly the dimples of transcrystalline ductile fracture. The fracture of the base material was propagated perpendicular to the direction of the tensile load. Within the dimples precipitated particles or impurities were observed.



a) b) c)

Figure 5. The morphology of fracture surface a) weld metal, b) heat affected zone, c) base material

Resistance to impact for samples of base material and laser welded for TRIP steel RAK 40/70 was evaluated by total deformation work [16]

$$W_{pl} = \frac{K.S_0.L_0.\left(\varphi_{max,necking} - \varphi_{0.002}\right)^{n+1}}{n+1} \quad (2)$$

from records of testing machine (Figure 6). In the equation (2) $\varphi_{max,necking}$ means the maximal deformation (strain) of the car body component, K is the material constant, n is the strain-hardening exponent, S_0 is the sample section and L_0 is the length of sample.

The support part of the car body shall be sufficiently strong and rigid to prevent plastic deformation of the body parts as a result of forces acting in normal operation, and only small plastic deformations of the parts are permitted in the event of an accident. The strength of the base material and the laser welded samples was determined [16]

$$\sigma_{dov,t} = \frac{R_{p0.2}}{k} = \sigma_{el} \quad (3)$$

and stiffness as the amount of elastic energy W_{el} that can absorb the material without plastic deformation of the part [16]

$$W_{el} = F.x_{\varepsilon<0.005} = \frac{R_e^2.S_0.L_0}{E.k^2} \quad (4)$$

where $R_{e0.005}$ is stress on elastic limit or $\sigma_{el} = E.\varepsilon_{el}$ at 0.005%.

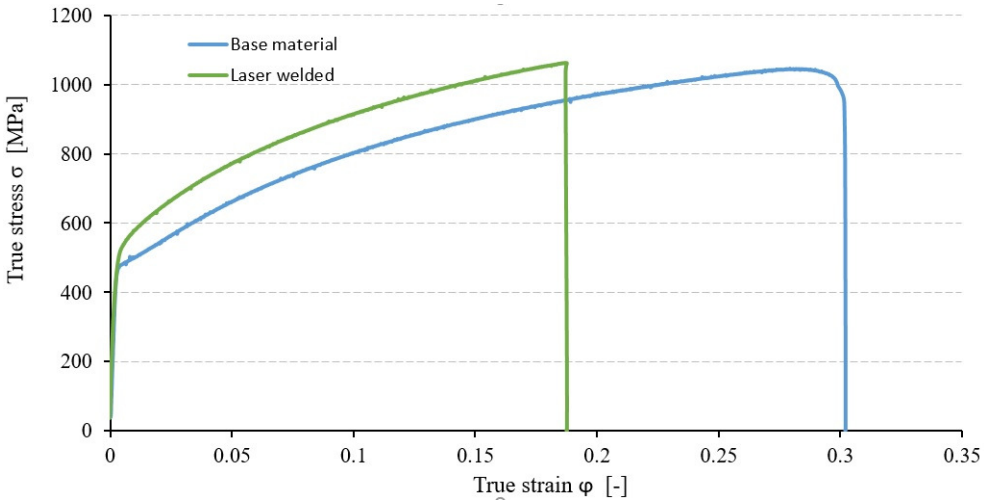


Figure 6. True stress – true strain diagram.

Similarly, it is possible to compare the stiffness and deformation work of the base material and the laser welded samples in the three-point bend test. From the record of the bending force dependence on the bend path it follows that it is a linear dependence [16]

$$F_{bend} = c.x \qquad [N] \quad (5)$$

where F_{bend} is bend force, c is the stiffness constant for defined samples shape, x is bending path or punch path. The slope of the bending force on the bend path determines the stiffness constant c – Figure 7.

Table 4. Measured and calculated values of deformation work and stiffness constant [15,16]

3-poind bend test								Tensile test			
BM				LW				BM		LW	
$F_{B\,max}$ [kN]	h_{max} [mm]	W [Nm]	c [MPa]	$F_{B\,max}$ [kN]	h_{max} [mm]	W [Nm]	c [MPa]	W_{el} [Nm]	E_{pl} [Nm]	W_{el} [Nm]	E_{pl} [Nm]
13.611	38.31	296.5	0.404	22.966	35.442	424.45	0.677	0.406	190	0.444	167

In Table 4 the calculated values of W_{el}, W_{pl} and strengths according to relations (2), (3), (4) are shown. As it comes out from the results of the tensile test, laser welded samples from TRIP steel RAK 40/70 showed 9% greater stiffness (W_{el}), 5% greater strength, 12% less overall deformation work than base material samples. However, at the same deformation φ = 0.19, the laser welded samples showed greater deformation work (W_{pl} = 157/144 = 1.09) by 9%.

The results of the three-point bend test showed that the stiffness constant is 67 % higher and the total deformation work is greater by 43 % for the base material. It is supposed, the higher values of the stiffness constant and deformation work at the same deformation are given by the more intense hardening of the material in the area of the weld metal and the heat-affected zone, due to the greater proportion of martensite in the welding joint structure than in the base material.

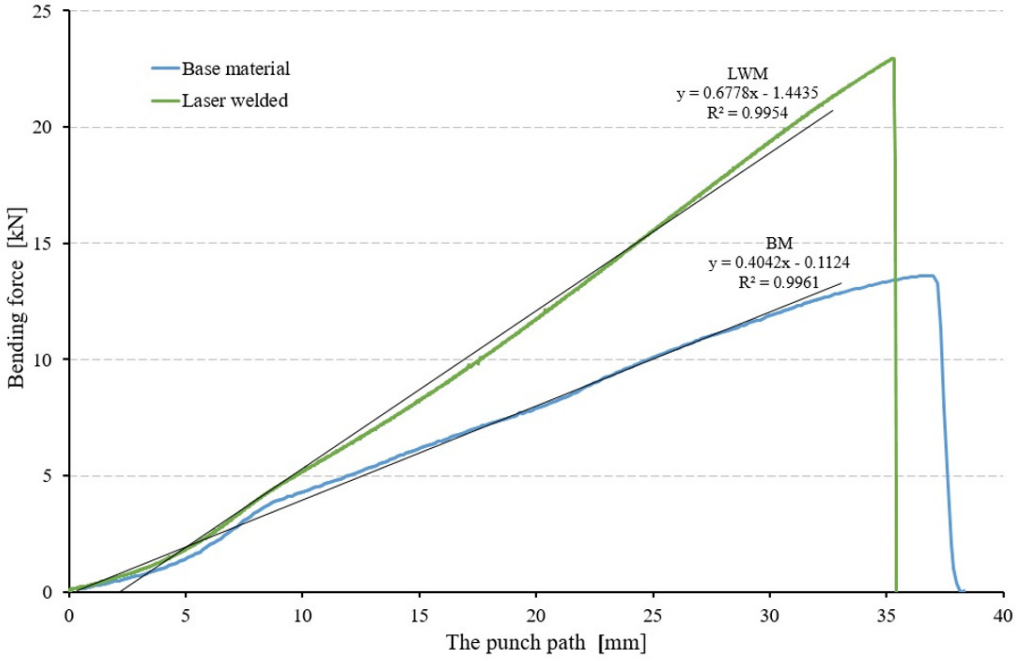


Figure 7. The bending force on the bend path dependence.

4. Conclusion

On the basis of the measured and analyzed results of the impact of laser welding by solid fiber lasers on the properties of TRIP steel sheets from RAK 40/70, it can be stated:

1. Based on the quality of the weld joint TRIP steel RAK 40/70 when laser welded by solid-state fiber laser YLS-5000 without protective gas in continuous welding mode it has been proved the most suitable mode with a welding speed of 50 mm.s^{-1} and power 2000 W.
2. The microstructure of the base material multi-phase TRIP steel RAK 40/70 consists of ferrite, very fine residual austenite, martensite and granular bainite. The microstructure in the heat-affected zone is heterogeneous, consisting of martensite and ferrite. As a result of laser welding, the proportion of martensite in the form of fine shapes of different forms decreases in the ferrite matrix from the center of the welding joint to the base material. The welding microstructure of the weld metal consists predominantly of fine martensite (formation in austenite grains) with random orientation of martensite laths.
3. Welded samples of multi-phase TRIP steel RAK 40/70 showed higher yield strength, lower tensile strength, tensibility, material constant K, and strain-hardening exponent n. The decrease in strength may be due to softening in the transition zone between the heat-affected zone and the base material or the result that the entire cross-section is not homogeneous. In the area of the weld metal, the largest proportion of martensite is in the form of larger islands, and its size as well as the size of its fragments decreases towards the base metal. We assume the strength and other properties depend not only on martensite share in the mixed structure but also on its morphology and distribution in structure.

4. Strength, stiffness and deformation work are important characteristics of the deformation process. From the results of the tensile test and the three-point bend test, a slight increase in strength, stiffness and deformation performance was observed for laser welded samples. In the area of the weld metal and the heat-affected zone, a greater proportion of martensite is present in the ferrite matrix in the form of fine shapes of different forms than in the base material, which makes the strainhardening contribution in this area larger than for the base material. Laser-welded samples showed a greater deformation strength effect than samples from the base material.
5. When comparing deformation work and stiffness, the amount of 10% plastic deformation is assumed for car body parts produced by forming or deformed at crash. Thus, for laser welded samples from multi-phase TRIP steel RAK 40/70, the WH effect increases the strength by 8%, the stiffness by 17%, deformation work at tensile by 12% (73.4 / 65.6 = 1.12), and at three-point bend test the stiffness constant and deformation increase by 67%.

Acknowledgments
The authors are grateful for the support of experimental works to Slovak Research and Development Agency, under project APVV-0273-12 "Supporting innovations of autobody components from the steel sheet blanks oriented to the safety, the ecology and the car weight reduction", as well as the grant agency for the support of the project VEGA 2/0113/16 "Influence of laser welding parameters on structure and properties of welded joints of advanced steels for the automotive industry".

References
[1] Incerti I, Walker A and Purton J 2010 *Paper to the International Bodyshop Industry Symposium* (Montreux, Switzerland) p. 1-9
[2] CO_2 emmisions change the material composition of vehicles and steel share decreases [online] 2014 [citted 2015-7-22] access: <http://www.cfo.sk/articles/emisie-co2-zmenia-materialovu-skladbu-automobilov-podiel-tradicnej-ocele-klesne#.VcDyMq2r07y>
[3] Jeanneau M and Pichant P 2000 *La Revue De Metallurgie* **97** 1399-1408
[4] Jacob G C, Fellers J F, Simunovic S and Starbuck J M 2002 *Journal of Composite Materials* **36** 813-850
[5] Zhang Ch, Song X, Lu P and Hu X 2012 *Materials & Design* **36** 233-242
[6] Mihaliková M and Lišková A. 2016 *Metalurgija* **55** 753-756
[7] Singh S, Nanda T, Ravi Kumar B and Singh V 2016 *Materials and Manufacturing Processes* **31** 2064-2075
[8] Švec P, Schrek A, Hrnčiar V and Csicsó T 2015 *Acta Metallurgica Slovaca* **21** 311-320
[9] Han Z Y, Zhang M D, Xu H F, Dong H and Cao W Q 2016 *Kang T'ieh/Iron and Steel* **51** 1-9
[10] Moravec J 2016 *25th International Conference on Metallurgy and Materials* (Brno, Czech Republic) p. 303-309
[11] Chen H, Yang Y and Wang L 2015 *Open Mechanical Engineering Journal* **9** 168-172
[12] Girman V and Hrabčáková V 2012 *Materials Engineer / Materiálový inžinier* 1-10
[13] Hall J N 2011 *Great Design in Steel Seminar* (USA: Livonia, Michigan)
[14] Hlavatý I 2001 *Weldability of steels* (Ostrava: ZERROS)
[15] Evin E and Tomáš M 2017 *Metals* **7** 239
[16] Evin E and Tomáš M 2017 *Final Report of the Project APVV-0273-12* (Košice: Technical University)